Kinetic Element Effect for Atropisomerization of an Organometallic Complex of the Misdirected Ligand 1,1′-Biisoquinoline†

Michael T. Ashby,* Susan S. Alguindigue, and Masood A. Khan

Department of Chemistry and Biochemistry, The University of Oklahoma, 620 Parrington Oval, Norman, Oklahoma 73019

Received October 18, 1999

The quinoline moieties of the metal-bound η^2-1,1′-biisoquinoline ligand of (η^6-benzene)(δ/λ-1,1′-biisoquinoline)halometal(II) hexafluorophosphate (metal = ruthenium, osmium; halo = chloro, iodo; **1**(M = Ru, Os; X = Cl, I)) are stereotopic. The rates of atropisomerization of the δ/λ-1,1′-biisoquinoline ligand, measured by spin-labeling NMR methods, indicate the energy barrier is higher for **1**(Ru) than **1**(Os); e.g., $\Delta H^{\ddagger}$[**1**(M = Ru, X = Cl)] = 77.3(2) and $\Delta H^{\ddagger}$[**1**(M = Os, X = Cl)] = 71.2(2) kJ mol^{-1}. Since the crystal structures of **1**(M = Ru, X = Cl) and **1**(M = Os, X = Cl) reveal comparable metric parameters, steric factors associated with atropisomerization of the 1,1′-biisoquinoline ligand, essentially the deformation of the 1,1′-binaphthylene skeleton that is necessary to pass H_8 and $H_{8'}$ past one another, are presumably equivalent for the Ru and Os derivatives. Assuming that normal bond energies are greater for the third-row transition metal than for second-row transition metals, we conclude the difference in reactivity can be attributed to electronic factors—the σ-donor orbitals and π-acceptor orbitals of the 1,1-biisoquinoline ligand are misdirected in the ground state but redirected in the *syn* transition state of atropisomerization. Thus, an inverse relationship between the kinetic and thermodynamic stabilities of **1** is observed for the misdirected ⇌ [directed]‡ ⇌ misdirected (MDM) isomerization of **1** (the more thermodynamically stable bond is more reactive). Atropisomerization of **1** represents only the second example of such an inverse free-energy relationship for a thermodynamically controlled reaction, and it contrasts with the regular relationship that has been found for the atropisomerization of related directed ⇌ [misdirected]‡ ⇌ directed (DMD) systems.

Downloaded by CARLI CONSORTIUM on June 29, 2009
Published on January 28, 2000 on http://pubs.acs.org | doi: 10.1021/om990825l

Introduction

We report herein the synthesis, solid-state structures, and studies of the dynamic behavior of the title compound (η^6-benzene)(δ/λ-1,1′-biisoquinoline)halometal(II) hexafluorophosphate (metal = ruthenium, osmium; halo = chloro, iodo; **1**(M = Ru, Os; X = Cl, I)). The 1,1′-biisoquinoline ligand of **1** is atropisomeric because of hindered rotation about the C_1−$C_{1'}$ bond as a result of steric conflict between H_8 and $H_{8'}$. We have previously reported a detailed mechanistic study of the diastereomerization of Δ/Λ-(δ/λ-1,1′-biisoquinoline)bis(2,2′-bipyridine)metal(II) (**2**(M = Ru, Os)) which demonstrated that interconversion of the two diastereomers proceeds via atropisomerization of the chiral 1,1′-biisoquinoline ligand (as shown in the diagram below) rather than epimerization of the chiral metal center.[1,2] We have furthermore suggested that the 1,1′-biisoquinoline ligand is misdirected in its ground-state conformation and its M−N bonds are bent. In the *syn* periplanar transition state **2**‡, the nitrogen σ-donor orbitals (and π-acceptor orbitals) of the ligand are presumably more effectively directed at the σ-acceptor orbitals (and π donor orbitals) of the metal. Since third-row transition metals typically form stronger bonds than their second-row congeners[3,4] and Ru compounds are generally more reactive than their Os derivatives,[5−8] the relatively more facile atropisomerization of **2**(M = Os) suggests the M−N bonds

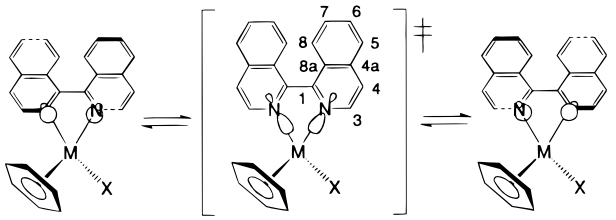

† Definitions: atropisomerization, hindered rotation about a single bond; misdirection, misalignment of donor−acceptor orbitals; directed, donor−acceptor orbitals that are aligned for optimal overlap; kinetic element effect, influence of replacing a second-row transition metal with a third-row transition metal on the rate of a reaction; inverse kinetic element effect, a third-row derivative reacts more rapidly than the corresponding second-row transition metal derivative.

(1) Ashby, M. T.; Govindan, G. N.; Grafton, A. K. *J. Am. Chem. Soc.* **1994**, *116*, 4801.
(2) Ashby, M. T. *J. Am. Chem. Soc.* **1995**, *117*, 2000.
(3) Ohanessian, G.; Goddard, W. A., III. *Acc. Chem. Res.* **1990**, *23*, 386.
(4) Martinho Simões, J. A.; Beauchamp, J. L. *Chem. Rev.* **1990**, *90*, 629.
(5) Pearson, J.; Cooke, J.; Takats, J.; Jordan, R. B. *J. Am. Chem. Soc.* **1998**, *120*, 1434.
(6) Halpern, J.; Cai, L. S.; Desrosiers, P. J.; Lin, Z. R. *J. Chem. Soc., Dalton Trans.* **1991**, 717.
(7) George, R.; Andersen, J. A. M.; Moss, J. R. *J. Organomet. Chem.* **1995**, *505*, 131.

10.1021/om990825l CCC: $19.00 © 2000 American Chemical Society
Publication on Web 01/28/2000

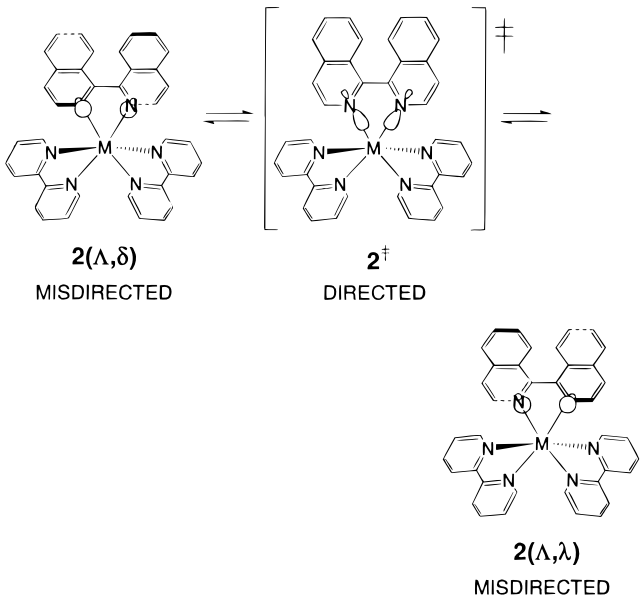

are weaker in the ground state than in the transition state of the atropisomerization. Thus, an inverse relationship exists between the thermodynamic and kinetic stabilities of **2** (the thermodynamically more stable Os derivative is kinetically more labile).[2]

We have sought to establish whether this trend is a general one for the 1,1′-biisoquinoline ligand: e.g., whether it is independent of the ancillary ligands that are involved. The C_2 symmetry of **2** renders the halves of their 1,1′-biisoquinoline ligands stereochemically equivalent. However, the metal centers of **2** are chiral by virtue of the fact they bear three bidentate ligands. Thus, compounds **2** are diastereomeric and, as our mechanistic study established, the rate of atropisomerization of the 1,1′-biisoquinoline ligand of **2** is related to the rate of diastereomerization, a process that can be followed by NMR spin-labeling techniques. Compounds **1** have only one chiral center and are enantiomeric, and their C_1 symmetry renders the halves of their 1,1′-biisoquinoline ligands stereochemically inequivalent. Thus, the rate of atropisomerization (epimerization) of **1** can be followed by measuring the rate of interconversion of the halves of their 1,1′-bisioquinoline ligands, again by NMR spin-labeling methods. Although there is no stereochemical handle to differentiate alternative isomerization mechanisms for **1**, we have recently demonstrated that the related complex (η^6-benzene)(δ/λ-1,1′-biphenyl-2,2′-diamine)chlorometal(II) hexafluorophosphate (metal = ruthenium, osmium; **3**(M = Ru, Os)) isomerizes via an atropisomerization barrier that

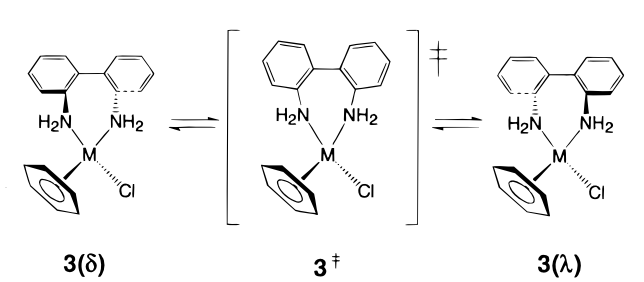

(8) Ashby, M. T.; Schwane, J. D.; Daniel, T. A. *Inorg. Chem.*, submitted for publication.

is comparable with that which we find for **1**.[9] We infer that the mechanisms for isomerization of **1** and **3** are the same, atropisomerization.

Because we have generally found larger entropic parameters for third-row metal derivatives compared to those for their second-row analogues, we have made a concerted effort to expand the temperature range over which kinetic data have been measured for **1**. This has been accomplished by employing both spin inversion transfer (SIT) and line-shape analysis (LSA) techniques. As was the case for **2**, we find the osmium derivative of **1** undergoes atropisomerization more rapidly than the ruthenium derivative. The present case of **1** represents only the second example of such an inverse free-energy relationship for a thermodynamically controlled (equilibrium) reaction.

Experimental Section

General Procedures. Acetone-d_6 was dried with molecular sieves and distilled before use. [(η^6-C_6H_6)$Ru(Cl)_2]_2$,[10] [(η^6-C_6H_6)-$Ru(I)_2]_2$,[10] [(η^6-C_6H_6)$Os(Cl)_2]_2$,[11] (η^6-C_6H_6)$Os(NCCH_3)(Cl)_2$,[12] and 1,1′-biisoquinoline (biiq)[1] were synthesized using literature methods. ^{1}H NMR spectra were recorded on a Varian XL-500 using residual acetone-d_5 (2.04 ppm) as an internal standard. The NMR samples were prepared in tubes that had been glass-blown onto Schlenk adapters. The solutions were freeze−pump−thawed, and the tubes were flame-sealed under vacuum. Combustion analyses were carried out by Midwest Microlab.

Synthesis of [(η^6-C_6H_6)Ru(biiq)(Cl)]PF_6 (1(M = Ru, X = Cl)). [(η^6-C_6H_6)$Ru(Cl)_2]_2$ (100 mg, 0.16 mmol) and 1,1′-biisoquinoline (150 mg, 0.59 mmol) were dissolved in MeOH (20 mL). The resulting solution was freeze−pump−thawed and left under vacuum, and the flask was placed in a 70 °C oil bath for 30 min. After the solution was cooled to room temperature, excess NH_4PF_6 (500 mg) was added to precipitate the product. The resulting yellow crystals were filtered, washed with MeOH, and dried under vacuum (215 mg, 87%). ^{1}H NMR (acetone-d_6, 500 MHz, 20 °C): δ 9.67 (d, $H_{3'}$, J = 6 Hz), 9.58 (d, H_3, J = 6 Hz), 8.39 (d, $H_{5'}$, J = 9 Hz), 8.38 (d, $H_{4'}$ J = 6 Hz), 8.34 (d, H_4, J = 6 Hz), 8.31 (d, H_5, J = 9 Hz), 8.13 (d, $H_{8'}$, J = 9 Hz), 8.08 (dd, $H_{6'}$, J = 8, 9 Hz), 8.00 (dd, H_6, J = 8, 9 Hz), 7.92 (d, H_8, J = 9 Hz), 7.82 (dd, $H_{7'}$, J = 8, 9 Hz), 7.70 (dd, H_7, J = 8, 9 Hz), 6.36 (s, 6H, arene). HRMS (FAB): *m/e* calcd for M^+ ($C_{24}H_{18}ClN_2Ru$), 471.0202; found, 471.0176 ± 0.026 (5 ppm error). Anal. Calcd for $C_{24}H_{18}ClF_6N_2PRu$: C, 46.80; H, 2.95. Found: C, 46.74; H, 3.11.

Synthesis of [(η^6-C_6H_6)Os(biiq)(Cl)]PF_6 (1(M = Os, X = Cl)). (η^6-C_6H_6)Os(acetonitrile)Cl_2 (75 mg, 0.19 mmol) and 1,1′-biisoquinoline (78 mg, 0.30 mmol) were mixed in degassed methanol (20 mL). The reaction mixture was freeze−pump−thawed, left under vacuum, and put into a 70 °C oil bath for 20 h. Excess NH_4PF_6 (500 mg) was added to precipitate the product. The product was filtered, washed with ether, and dried under vacuum (81 mg, 60%). ^{1}H NMR (acetone-d_6, 500 MHz, 20 °C): δ 9.64 (d, $H_{3'}$, J = 6 Hz), 9.62 (d, H_3, J = 6 Hz), 8.41 (d, $H_{5'}$, J = 9 Hz), 8.35 (d, H_5, J = 9 Hz), 8.34 (d, $H_{4'}$, J = 6 Hz), 8.33 (d, H_4, J = 6 Hz), 8.23 (d, $H_{8'}$, J = 9 Hz), 8.09 (dd, $H_{6'}$, J = 8, 9 Hz), 8.08 (d, H_8, J = 9 Hz), 8.01 (dd, H_6, J = 8, 9 Hz), 7.85 (dd, $H_{7'}$, J = 8, 9 Hz), 7.77 (dd, H_7, J = 8, 9 Hz), 6.50 (s, 6H, arene). HRMS (FAB): *m/e* calcd for M^+ ($C_{24}H_{18}ClN_2$-Os), 561.0773; found, 561.0752 ± 0.021 (5 ppm error). Anal. Calcd for $C_{24}H_{18}ClF_6N_2POs$: C, 40.89; H, 2.58. Found: C, 40.35; H, 2.61.

(9) Alguindigue, S. S.; Khan, M. A.; Ashby, M. T. *Organometallics* **1999**, *18*, 5112.
(10) Zelonka, R. A.; Baird, M. C. *Can. J. Chem.* **1972**, *50*, 3063.
(11) Arthur, T.; Stephenson, T. A. *J. Organomet. Chem.* **1981**, *208*, 369.
(12) Freedman, D. A.; Magneson, D. J.; Mann, K. R. *Inorg. Chem.* **1995**, *34*, 2617.

Downloaded by CARLI CONSORTIUM on June 29, 2009
Published on January 28, 2000 on http://pubs.acs.org | doi: 10.1021/om990825l

Downloaded by CARLI CONSORTIUM on June 29, 2009
Published on January 28, 2000 on http://pubs.acs.org | doi: 10.1021/om990825l

Table 1. Crystal Data and Structure Refinement for 1(M = Ru, X = Cl) and 1(M = Os, X = Cl)

	1(M = Ru, X = Cl)	**1**(M = Os, X = Cl)
empirical formula	$C_{24}H_{18}ClF_6N_2PRu$	$C_{24}H_{18}ClF_6N_2POs$
fw	615.89	705.02
space group	$P\bar{1}$	$P\bar{1}$
cryst syst	triclinic	triclinic
a, Å	9.9564(7)	9.980(1)
b, Å	10.9510(7)	10.9302(9)
c, Å	11.2730(11)	11.264(2)
α, deg	102.009(7)	101.98(1)
β, deg	93.963(7)	94.186(9)
γ, deg	110.276(6)	110.157(7)
V, Å^3	1114.3(2)	1114.2(2)
T, K	188(2)	173(2)
Z	2	2
D_{calcd}, mg cm^{-3}	0.836	2.101
μ, mm^{-1}	1.963	5.981
cryst size, mm^3	0.32 × 0.64 × 0.32	0.12 × 0.34 × 0.32
no. of indep rflns	4795	4301
θ range (deg)	1.87−26.99	1.87−26.00
final *R* indices	R1 = 0.0282	R1 = 0.0256
($I > 2\sigma(I)$)	wR2 = 0.0759	wR2 = 0.0637
R indices (all data)	R1 = 0.0294	R1 = 0.0286
	wR2 = 0.07887	wR2 = 0.0660
GOF	1.106	1.057

Synthesis of [(η^6-C_6H_6)Ru(biiq)(I)]PF_6 (1(M = Ru, X = I)). [(η^6-C_6H_6)RuI_2]$_2$ (82 mg, 0.10 mmol) and 1,1′-biisoquinoline (25 mg, 0.10 mmol) were dissolved in MeOH (20 mL). The resulting solution was freeze−pump−thawed, left under vacuum, and put into a 70 °C oil bath for 1 h. After the mixture was cooled to room temperature, excess NH_4PF_6 (500 mg) was added to precipitate the product. The resulting red product was filtered and dried under vacuum (27 mg, 84%). ^{1}H NMR (acetone-d_6, 500 MHz, 20 °C): δ 9.58 (d, $H_{3'}$, J = 6 Hz), 9.55 (d, H_3, J = 6 Hz), 8.39 (d, $H_{5'}$, J = 9 Hz), 8.34 (d, $H_{4'}$, J = 6 Hz), 8.30 (d, H_5, J = 9 Hz), 8.28 (d, H_4, J = 6 Hz), 8.13 (d, $H_{8'}$, J = 9 Hz), 8.06 (dd, $H_{6'}$, J = 8, 9 Hz), 8.00 (dd, H_6, J = 8, 9 Hz), 7.95 (d, H_8, J = 9 Hz), 7.82 (dd, $H_{7'}$, J = 8, 9 Hz), 7.71 (dd, H_7, J = 8, 9 Hz), 6.43 (s, 6H, arene). GC-HRMS (FAB): *m*/*e* calcd for M$^+$ ($C_{24}H_{18}IN_2Ru$), 562.9558; found, 562.9562 ± 0.004 (1 ppm error).

Synthesis of [(η^6-C_6H_6)OsI_2]$_2$. The following procedure is essentially the same as that previously used to synthesize [(η^6-C_6H_6)RuI_2]$_2$.[10] [(η^6-C_6H_6)$OsCl_2$]$_2$ (93 mg, 0.14 mmol) was dissolved in 95% EtOH by stirring for 2 h. Excess NaI (500 mg) was added, and the resulting solution was stirred overnight. The brown precipitate was filtered, washed with water, and dried under vacuum (77 mg). The product was used without further purification in the synthesis of **1**(M = Os, X = I).

Synthesis of [(η^6-C_6H_6)Os(biiq)(I)]PF_6 (1(M = Os, X = I)). [(η^6-C_6H_6)OsI_2]$_2$ (77 mg, 0.07 mmol) and 1,1′-biisoquinoline (35 mg, 0.14 mmol) were dissolved in acetonitrile (20 mL). The resulting solution was freeze−pump−thawed, left under vacuum, and put into a 70 °C oil bath for 19 h. After the mixture was cooled to room temperature, excess NH_4PF_6 (500 mg) was added and the solvent removed under vacuum. The residue was dissolved in CH_2Cl_2 and filtered to remove a white impurity. The CH_2Cl_2 was removed on a rotary evaporator and the red product dried under vacuum. Yield: 66 mg, 56%. ^{1}H NMR (acetone-d_6, 500 MHz, 20 °C): δ 9.57 (d, $H_{3'}$, J = 6 Hz), 9.54 (d, H_3, J = 6 Hz), 8.38 (d, $H_{5'}$, J = 9 Hz), 8.32 (d, H_5, J = 9 Hz), 8.25 (d, 2H, $H_{4,4'}$, J = 6 Hz), 8.21 (d, $H_{8'}$, J = 9 Hz), 8.07 (d, H_8, J = 9 Hz), 8.03 (dd, $H_{6'}$, J = 8,9 Hz), 7.98 (dd, H_6, J = 8, 9 Hz), 7.83 (dd, $H_{7'}$, J = 8, 9 Hz), 7.75 (dd, H_7, J = 8, 9 Hz), 6.55 (s, 6H, arene). HRMS (FAB): *m*/*e* calcd for M$^+$ ($C_{24}H_{18}IN_2Os$), 653.0130; found, 653.0101 ± 0.029 (4 ppm error).

X-ray Diffraction Study of 1(M = Ru, X = Cl) and 1(M = Os, X = Cl). Crystallographic solution and refinement procedures are summarized in Table 1. Diffraction-quality crystals were grown by vapor diffusion of ether into a solution of **1** in acetone. A Siemens P4 four-circle diffractometer was employed to collect a $\theta/2\theta$ data set at 188 K for **1**(M = Ru, X = Cl) and 173 K for **1**(M = Os, X = Cl) using Mo Kα radiation (0.710 73 Å).[13] The data were corrected for Lorentz and polarization effects, and an empirical absorption correction based on ψ-scans was applied.[14] The structure was solved by the heavy-atom method, using the Siemens SHELXTL system, and refined by full-matrix least squares on F^2 using all of the reflections.[15] All of the non-hydrogen atoms were refined anisotropically, and all of the hydrogen atoms were included in the refinement at geometrically idealized positions with fixed temperature factors. Disorder of the arene ligand of **1**(M = Ru, X = Cl) was adequately treated by a two-site model with equal occupancy. Atomic coordinates and isotropic vibrational parameters for **1**(M = Ru, X = Cl) and **1**(M = Os, X = Cl) are given in the Supporting Information. Selected interatomic distances, angles, and torsion angles are given in Table 2. A diagram showing the thermal ellipsoids (at the 50% level) of the molecule and labeling scheme for **1**(M = Ru, X = Cl) is given in Figure 1. A similar figure for **1**(M = Os, X = Cl) is available in the Supporting Information.

Assignment of ^{1}H NMR Spectrum of 1. Scalar coupling relationships between the protons were obtained using ^{1}H−^{1}H double-quantum-filtered homonuclear correlation spectroscopy (dqf-COSY)[16] for all of the derivatives of **1**. A representative COSY spectrum for **1**(M = Ru, X = Cl) is available in the Supporting Information (Figure S2). Similar spectra were obtained for the other derivatives of **1**. The subsequent assignment of the proton resonances were made on the basis of our experience with other metal complexes of 1,1′-biisoquinoline that have both C_1 and C_2 symmetry[1,2,8] and the assumption that $H_{3,3'}$ versus $H_{4,4'}$ and $H_{8,8'}$ versus $H_{5,5'}$ are going to exhibit the largest differences in chemical shift.

Despite the fact that the peaks we assign as $H_{8,8'}$ exhibited the largest difference in chemical shift, one or both of these peaks were obscured by other resonances in most of the derivatives of **1**. The most cleanly separated resonances corresponded to $H_{7,7'}$, which were the peaks that were irradiated in the spin-labeling experiments. It is important to note that, unlike similar studies we have carried out,[1,2,8,9] there is no stereochemical handle that allows us to differentiate between different mechanisms that could give rise to magnetic exchange of the halves of the 1,1′-biisoquinoline ligand of **1** (vide infra). Since no additional insight into the mechanism is garnered from the spin-labeling NMR experiments, correct assignment of the ^{1}H NMR spectra of **1** is not critical.

Symmetry of Magnetic Exchange by 2D EXSY. The two-dimensional exchange spectroscopy (2D EXSY) pulse sequence and the experimental procedure used to carry out these experiments have been described in detail elsewhere.[17] The spectrum of Figure 2 for **1**(M = Ru, X = Cl) only illustrates the positive peaks; therefore, the cross-peaks corresponding to chemical exchange are observed. Relatively small negative NOE peaks were also observed in the 2D EXSY spectra. Similar spectra were obtained for the other derivatives of **1**.

Rates of Atropisomerization by Spin Inversion Transfer (SIT) NMR. SIT rate data were obtained using the standard pulse sequence[18−21] and methods that have been

(13) XSCANS: X-ray Single-Crystal Analysis System; Siemens Analytical X-ray Instruments Inc., Madison, WI, 1994.
(14) North, A. C. T.; Phillips, D. C.; Mathews, F. S. *Acta Crystallogr.* **1968**, *A24*, 351.
(15) SHELXTL Software Package for the Determination of Crystal Structures; Siemens Analytical X-ray Instruments, Inc., Madison, WI, 1995.
(16) Rance, M.; Sorensen, O. W.; Bodenhausen, G.; Wagner, G.; Ernst, R. R.; Wüthrich, K. *Biochem. Biophys. Res. Commun.* **1983**, *117*, 479.
(17) Abel, E. W.; Coston, T. P. J.; Orrell, K. G.; Sik, V.; Stephenson, D. *J. Magn. Reson.* **1986**, *70*, 34.
(18) Alger, J. R.; Prestegard, J. H. *J. Magn. Reson.* **1977**, *27*, 137.
(19) Kuchel, R. W.; Chapman, B. E. *J. Theor. Biol.* **1983**, *105*, 569.
(20) Bellon, S. F.; Chen, D.; Johnston, E. R. *J. Magn. Reson.* **1987**, *73*, 168.

previously described.[9] Typical fits for spin transfer and inversion recovery are illustrated in Figure S3. The kinetic data (k_{obs}'s) that were obtained from the SIT experiments and the conditions that were employed for each experiment are summarized in Table 3 for **1**(M = Ru, Os; X = Cl) and Table 4 for **1**(M = Ru, Os; X = I).[22]

Rates of Atropisomerization by NMR Line-Shape Analysis (LSA). It was possible to measure the rates of atropisomerization of **1**(M = Ru, Os; X = I) by LSA, thereby increasing the temperature range over which kinetic data could be analyzed by an Eyring plot (Figure 4). Similar analysis of the chloride series was not possible because **1**(M = Ru, Os; X = Cl) decomposes well below the coalescence temperature of its NMR spectrum. Although the decomposition products were not fully characterized, their NMR spectra suggested solvolysis of the halide ligand of **1**. For **1**(M = Ru, Os; X = I), $H_3/H_{3'}$ coalesce at 79 °C for M = Os and 93 °C for M = Ru. LSA was carried out using the FORTRAN program DNMR5 running on a Silicon Graphics IRIS Indigo X24.[23] The kinetic data (k_{obs}'s) that were obtained from the LSA experiments and the conditions that were employed for each experiment are summarized in Table 4 for **1**(M = Ru, Os; X = I). Rate data that were collected over an intermediate temperature range which permitted application of both SIT and LSA were in good agreement.

Results and Discussion

Solution and Solid-State Structures of 1(M = Ru, X = Cl) and 1(M = Os, X = Cl). The nonplanar nature of the 1,1′-binaphthylene ring system formed by the 1,1′-biisoquinoline ligand renders **1** chiral (C_1 symmetry). This is clearly seen in the solid state, as determined by single-crystal X-ray crystallography (Figure 1). The molecular structures of **1** may be compared with related structures. The observed Ru−N interatomic distance of 2.08 Å for **1**(M = Ru) is not extraordinary. For compounds with the formula $[(\eta^6\text{-arene})Ru(Cl)(N)_2]^+$, imine (2.08 Å)[24] and nitrile donors (2.06 Å)[25] tend to have shorter Ru−N bonds, whereas amine donors (2.13−2.18 Å)[9,26] have longer bonds. The Ru−N bonds that have been observed for pyridine-type donor complexes analogous to **1** range from 2.09 to 2.17 Å.[24,27−29] Thus, the Ru−N bond lengths that are observed for **1**(M = Ru, X = Cl) are on the short end of the scale for all $[(\eta^6\text{-arene})Ru(Cl)(N)_2]^+$ complexes, which may reflect an effort to improve overlap between the Ru and the misdirected 1,1′-biisoquinoline ligand. The N−C−C′−N′ torsional angles of 27.0° for **1**(M = Ru, X = Cl) and 25.6° for **1**(M = Os, X = Cl) fall within the range of 20.1−26.4° that has been found for five other (η^2-1,1′-biisoquinoline)-metal complexes.[1,2,30,31] It is interesting that, in both of the systems for which we have crystal structures of the Ru and Os derivatives, the third-row derivatives have somewhat more acute N−Cl−Cl′−N′ torsion angles than the second-row derivatives; 27.0/25.6° and 24.1/20.1° for **1**(M = Ru, X = Cl)/**1**(M = Os, X = Cl) and **2**(M = Ru)/**2**(M = Os), respectively. This may indicate that the inherently stronger Os−N bonds are able to overcome the interatomic repulsion of $H_8/H_{8'}$ to a larger extent. The other metric data for **1** are unremarkable. The C_1 symmetry of **1** is maintained in solution on the

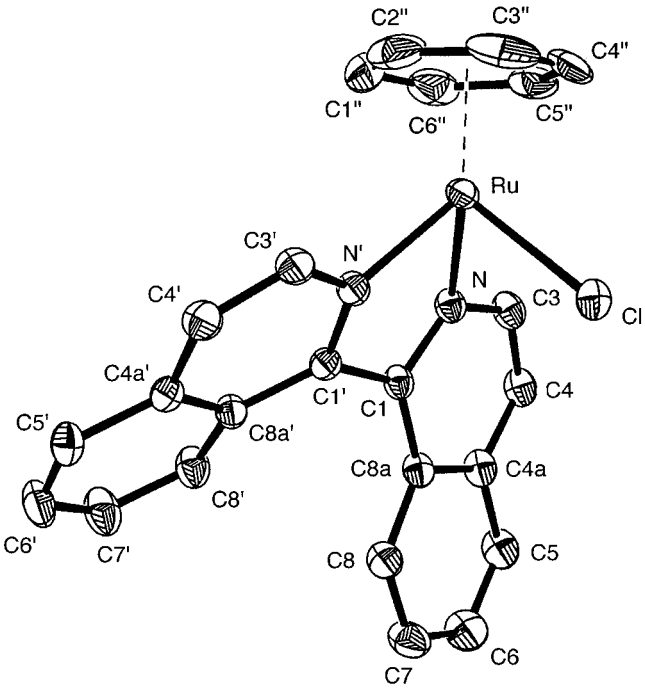

Figure 1. Molecular structure of **1**(M = Ru, X = Cl) showing the atom-labeling scheme and the thermal vibration ellipsoids (50% probability). A similar figure is available for **1**(M = Os, X = Cl) in the Supporting Information (Figure S1).

Table 2. Comparison of Selected Interatomic Distances (Å), Angles (deg), and Torsion Angles (deg) for 1(M = Ru, X = Cl) and 1(M = Os, X = Cl)[a]

	M = Ru	M = Os
M−N	2.087(2)	2.085(3)
M−N′	2.085(2)	2.086(3)
M−Cl	2.388(1)	2.392(1)
$M-Ar_{cent}(1)$	1.679(4)	1.675(3)
$M-Ar_{cent}(2)$	1.682(4)	
N−M−N′	76.38(6)	75.9(1)
N−M−Cl	82.0(1)	81.40(9)
N′−M−Cl	87.4(1)	86.59(9)
$N-M-Ar_{cent}(1)$	132.9(2)	132.7(1)
$N-M-Ar_{cent}(2)$	132.6(2)	
$N'-M-Ar_{cent}(1)$	132.0(2)	131.3(1)
$N'-M-Ar_{cent}(2)$	128.7(2)	
$Cl-M-Ar_{cent}(1)$	127.5(1)	129.5(1)
$Cl-M-Ar_{cent}(2)$	130.8(1)	
N−C1−C1′−N′	27.0(2)	25.5(4)

[a] Ar is defined to be the least-squares plane that contains an arene ligand. $Ar_{cent}(1)$ is the centroid of the arene ligand C1″−C6″ for M = Ru and M = Os. $Ar_{cent}(2)$ is the centroid of the arene ligand C1‴−C6‴ for M = Ru.

(21) Robinson, G.; Kuchel, P. W.; Chapman, B. E. *J. Magn. Reson.* **1985**, *63*, 314.
(22) Green, M. L. H.; Wong, L.-L.; Sella, A. *Organometallics* **1992**, *11*, 2660.
(23) Stephenson, D. S.; Binsch, G. DNMR5: Iterative Nuclear Magnetic Resonance Program for Unsaturated Exchange-Broadened Band Shapes; Institute of Organic Chemistry, University of Munich, Munich, FRG (QCPE 365).
(24) Mandal, S. K.; Chakravarty, A. R. *Polyhedron* **1992**, *11*, 823.
(25) McCormick, F. B.; Cox, D. D.; Gleason, W. B. *Organometallics* **1993**, *12*, 610.
(26) Gould, R. O.; Jones, C. L.; Robertson, D. R.; Stephenson, T. A. *Cryst. Struct. Commun.* **1978**, *7*, 27.
(27) Davies, D. L.; Fawcett, J.; Garvatt, S. A.; Russell, D. R. *J. Chem. Soc., Chem. Commun.* **1997**, 1351.
(28) Elsegood, M. R. J.; Tocher, D. A. *J. Organomet. Chem.* **1988**, *356*, C29.
(29) Mosny, K. K.; de Gala, S. R.; Crabtree, R. H. *Transition Met. Chem.* **1995**, *20*, 595.
(30) Cheng, L.-K.; Yeung, K.-S.; Che, C.-M.; Cheng, M.-C.; Wang, Y. *Polyhedron* **1993**, *12*, 1201.
(31) Ashby, M. T.; Manke, I. A.; Khan, M. A. Unpublished crystal structure of $[Ir(bipy)_2(biiq)]^{3+}$.

Downloaded by CARLI CONSORTIUM on June 29, 2009
Published on January 28, 2000 on http://pubs.acs.org | doi: 10.1021/om990825l

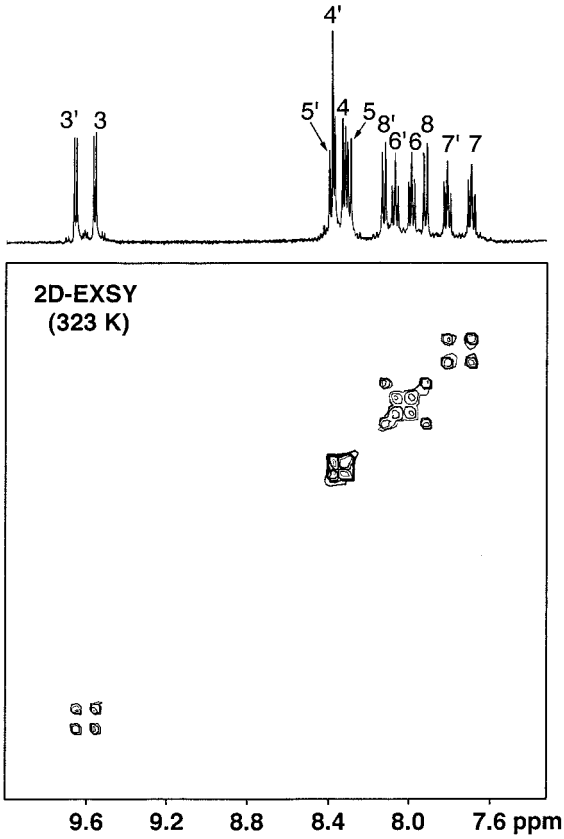

Figure 2. 2D-EXSY spectrum for **1**(M = Ru, X = Cl) at 323 K and 500 MHz that illustrates pairwise chemical exchange. The corresponding 2D-COSY spectrum for **1**(M = Ru, X = Cl) at 323 K and 500 MHz is available in the Supporting Information (Figure S2).

NMR time scale, as evidenced by the inequivalent chemical shifts observed for the halves of the 1,1′-biisoquinoline ligand. However, stereochemical exchange on the spin-relaxation time scale is evidenced by spin perturbation studies (vide infra).

Dynamic Behavior of 1(M = Ru, X = Cl) in Solution. Spin-perturbation NMR methods reveal pairwise exchange of the halves of the 1,1′-biisoquinoline ligand in acetone solution (Figure 2). The exchange behavior is further evidenced at higher temperatures, where coalescence is observed (Figure 3). There are several conceivable mechanisms that could account for such magnetic exchange. Isomerization of the ligand is possible through atropisomerization via a *syn* or an *anti* transition state. The latter would require the cleavage of one of the M−N bonds to form a nascent η^1-1,1′-biisoquinoline species. Alternatively, exchange of the stereochemical roles of the η^6-C_6H_6 and Cl ligands ("inversion" at the metal) is possible through either an intramolecular or intermolecular process (e.g., through dissociation of Cl^-). Previous studies we have carried out for 1,1′-biisoquinoline complexes have allowed us to differentiate between such mechanisms. In every case, atropisomerization of an η^2-1,1′-biisoquinoline ligand through a *syn* transition state was inferred.[1,2,8] In our recent study of the atropisomerization of the 1,1′-biphenyl-2,2′-diamine (dabp) ligand of $[(\eta^6\text{-}C_6H_6)M(dabp)Cl]^+$ (**4**(M = Ru, Os)), the metal inversion mechanism could be ruled out on the basis of symmetry arguments.[9] We therefore conclude that the magnetic exchange observed for **1** is due to atropisomerization of the 1,1′-biisoquinoline ligand via a *syn* periplanar transition state.

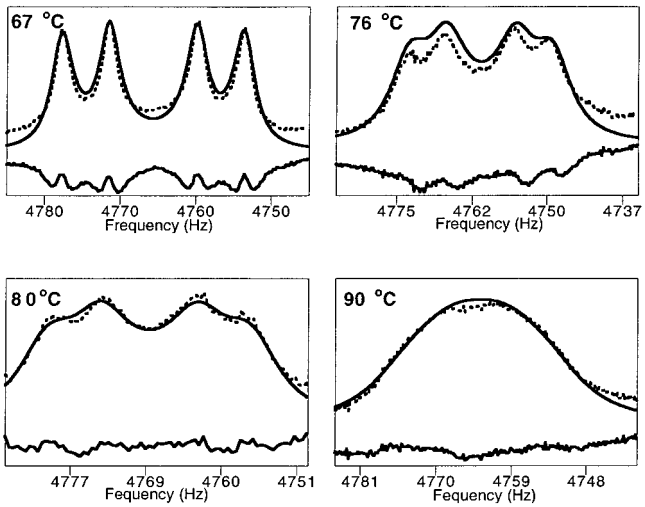

Figure 3. Line-shape analysis (LSA) for **1**(M = Ru, X = Cl) at 500 MHz.

Table 3. Comparison of the Kinetic Data Obtained for the Atropisomerization of 1(M = Ru, X = Cl) and 1(M = Os, X = Cl)

	k_1 (s^{-1})			k_1 (s^{-1})	
temp (°C)	M = Ru	M = Os	temp (°C)	M = Ru	M = Os
21		0.36(1)	41	1.78(1)	2.24(3)
24	0.292(3)	0.439(3)	46	2.71(1)	3.48(2)
29	0.456(5)	0.820(7)	51	4.11(1)	5.54(4)
34	0.703(7)	1.07(1)	55	5.78(3)	7.66(7)
38	1.09(1)				

Table 4. Comparison of the Kinetic Data Obtained for the Atropisomerization of 1(M = Ru, X = I) and 1(M = Os, X = I)

	k_1 (s^{-1})			k_1 (s^{-1})	
temp (°C)	M = Ru	M = Os	temp (°C)	M = Ru	M = Os
38	0.467(8)[a]	0.82(1)[a]	66		8.2(6)[b]
43	0.76(2)[a]	1.36(1)[a]	67	6.3(1)[b]	
48	1.16(1)[a]	1.71(1)[a]	70		11.5(8)[b]
53	1.57(2)[a]	3.24(3)[a]	75		17(1)[b]
57	2.72(3)[a]		76	11.2(7)[b]	
59		4.86(6)[a]	80	15.6(6)[b]	
61		5.8(1)[b]	90	32.3(6)[b]	
62	4.33(2)[a]				

[a] Measured by spin inversion transfer. [b] Measured by line-shape analysis.

Ligand Misdirection. As we have done previously for related systems,[2,8] it is interesting to compare the kinetics of atropisomerization of **1**(M = Ru) with **1**(M = Os) (Tables 3 and 4). We have previously shown that atropisomerization of the 1,1′-biisoquinoline ligand complexes of Ru and Os exhibit an inverse free-energy relationship (Os with its stronger metal−ligand bonds undergoes atropisomerization more readily).[2] This trend is attributed to a strengthening of the metal−biisoquinoline bonds in the *syn* transition state of atropisomerization. In contrast, isomerization reactions that involve a weakening of metal−ligand bonds result in a regular free-energy relationship (Ru faster than Os).[8] We have previously referred to such comparisons between second-row-metal and third-row-metal derivatives "Kinetic Element Effects".[8] We find for **1** a significant difference between the rates of atropisomerization of the Ru and Os derivatives. As for other

Downloaded by CARLI CONSORTIUM on June 29, 2009
Published on January 28, 2000 on http://pubs.acs.org | doi: 10.1021/om990825l

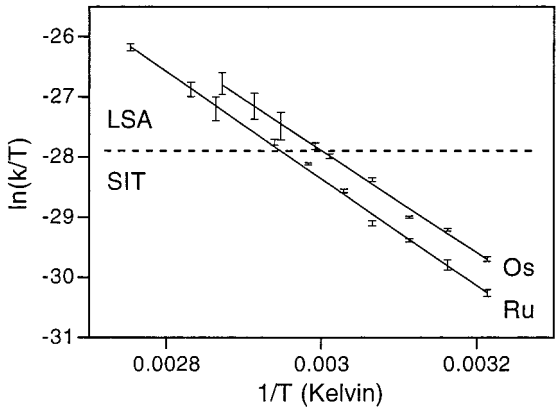

Figure 4. Eyring plot of the rate data of Table 4 for **1**(M = Ru, Os; X = I). The error bars reflect 3 times the estimated standard deviation of the rate constants. Data below the dashed line were obtained by SIT and those above the line by LSA.

atropisomerization reactions of metal complexes of 1,1′-biisoquinoline complexes, we find the second-row-metal is slower than the third-row-metal derivative.It stands to reason that if the difference in reactivity of the Ru and Os derivatives of **1** is due to bond perturbation effects, the origin should lie in the enthalpy of activation. Furthermore, we have generally found larger entropic parameters for third-row-metal derivatives compared to their second-row analogues for atropisomerization of metal complexes for 1,1′-biisoquinoline. Accordingly, we have expanded the temperature range over which kinetic data have been measured for **1** to permit more accurate determination of the activation parameters. This was accomplished by employing both spin inversion transfer (SIT) and line-shape analysis (LSA) techniques. For reasons discussed earlier, LSA was only possible for **1**(X = I) (Table 4). The kinetic data that were obtained by SIT and LSA were in good agreement, as evidenced by the Eyring plot of Figure 4. The activation parameters that were determined for **1**(X = Cl) (SIT only) and **1**(X = I) (SIT and LSA) are summarized in Table 5. As expected, perhaps, the results for **1**(X = Cl) and **1**(X = I) are comparable. While the difference in Gibbs free energy of activation ($\Delta\Delta G^{\ddagger}$) for the Ru and Os derivatives amounts to only about 1 kJ mol^{-1} in favor of Os, the difference in enthalpy of activation ($\Delta\Delta H^{\ddagger}$) is about 6 kJ mol^{-1}, again in favor of Os. Once more, we observe more negative entropies of activation for the Os derivatives. Although the origin of the difference of entropies of activation is not clear, all fall within the range that is typically observed for unimolecular reactions.

Table 5. Comparison of the Activation Parameters Obtained for Atropisomerization of 1(M = Ru) and 1(M = Os)

	M, X			
	Ru, Cl	Os, Cl	Ru, I	Ru, I
$\Delta H^{\ddagger}$ (kJ/mol)	77.3(2)	71.2(2)	76.5(3)	70.2(5)
$\Delta S^{\ddagger}$ (J/(K mol))	4.8(7)	−11.6(7)	−5(1)	−21(1)
$\Delta G^{\ddagger}_{50}$ (kJ/mol)	75.8	75.0	78.4	77.1

Conclusions

We conclude that the mechanism of isomerization of (η^6-benzene)(δ/λ-1,1′-biisoquinoline)halometal(II) hexafluorophosphate (**1**; metal = ruthenium, osmium, halo = chloro, iodo) is inversion of stereochemistry at the 1,1′-biisoquinoline ligand center via a *syn* transition state. The observed inverse Kinetic Element Effect (KEE) indicates a strengthening of the M−N bonds of **1** in the transition state of atropisomerization relative to the ground state. To our knowledge, this is only the second time an inverse free-energy relationship has been demonstrated for a thermodynamically controlled (equilibrium) reaction.

Acknowledgment. The financial support of the National Science Foundation (Grant No. CHE-9612869) and the donors of the Petroleum Research Fund, administered by the American Chemical Society, is gratefully acknowledged. S.S.A. is a Department of Education GAANN Fellow.

Supporting Information Available: Tables of the crystallographic data (fractional coordinates of all atoms, anisotropic displacement parameters for the non-hydrogen atoms, bond distances and bond angles) for **1**(M = Ru, X = Cl) and **1**(M = Os, X = Cl), a thermal ellipsoid plot of **1**(M = Os, X = Cl), a COSY NMR spectrum of **1**(M = Ru, X = Cl), and an SIT fit of **1**(M = Ru, X = Cl) at 46 °C. This material is available free of charge via the Internet at http://pubs.acs.org.

OM990825L

Downloaded by CARLI CONSORTIUM on June 29, 2009
Published on January 28, 2000 on http://pubs.acs.org | doi: 10.1021/om990825l